

Zero modes of various graphene configurations from the index theorem

Jiannis K. Pachos^{1,a}, Agapitos Hatzinikitas², and Michael Stone³

¹ School of Physics and Astronomy, University of Leeds, Leeds LS2 9JT, UK

² Department of Statistics and Actuarial-Financial Mathematics, School of Sciences, University of Aegean, 83200 Samos, Greece

³ Department of Physics, University of Illinois, 1110 W. Green St. Urbana, IL 61801, USA

Abstract. In this article we consider a graphene sheet that is folded in various compact geometries with arbitrary topology described by a certain genus, g . While the Hamiltonian of these systems is defined on a lattice one can take the continuous limit. The obtained Dirac-like Hamiltonian describes well the low energy modes of the initial system. Starting from first principles we derive an index theorem that corresponds to this Hamiltonian. This theorem relates the zero energy modes of the graphene sheet with the topology of the compact lattice. For $g = 0$ and $g = 1$ these results coincide with the analytical and numerical studies performed for fullerene molecules and carbon nanotubes while for higher values of g they give predictions for more complicated molecules.

1 Introduction

The spectrum of graphene and its various geometrical configurations has been the focus of extensive study [1,2,3,4,5,6]. It provides a physical system where a unique interplay is witnessed between geometry and electronic properties such as conductivity. Nevertheless, a unified picture has not been derived so far due to the richness in behavior of the various geometrical configurations as well as the difficulty in approaching them analytically. One of the interests is to study the number of electronic eigenstates with zero energy that determine the conductivity of the system and its ground state degeneracy. Previous methods for obtaining the zero modes of the system are based on lengthy analytical or numerical procedures. As a possible alternative the much celebrated index theorem [7] offers an analytic tool that relates the zero modes of elliptic operators with the geometry of the manifold on which these operators are defined. This theorem has a dramatic impact on theoretical and applied sciences [8]. It provides information about the spectrum of widely used elliptic operators based on simple geometric considerations that could be otherwise hard or even impossible to determine.

In this article we would like to describe the effect geometrical deformations have on the spectrum of graphene. For that we shall establish a version of the index theorem [7,8,9] that relates the number of zero modes of graphene wrapped on arbitrary compact surfaces to the topology of the surface. In our pursue we shall ignore changes in the couplings caused by the geometrical deformations and we shall focus only on the effect the geometry has on the spectrum of graphene. As we shall see our results are in good agreement with the known cases of icosahedral fullerene molecules [10] and graphite nanotubes [11] where the spectrum has been determined analytically or numerically. Similar approaches for the ground state degeneracy of fractional quantum Hall systems in the planar case or on high-genus Riemannian surfaces have been taken in [12,13,14,15,16].

^a e-mail: j.k.pachos@leeds.ac.uk

2 The graphene sheet

First we shall present an overview of the properties of a flat sheet of graphene. When considering its low energy limit a linearization of the energy is possible due to the presence of individual Fermi points in the spectrum. This results in a Dirac equation [3], which describes well the low energy behavior of the system.

Graphene consists of a two dimensional honeycomb lattice where Carbon atoms occupy its vertices. When we adopt the tight-binding approximation the model reduces the system of coupled fermions on a honeycomb lattice [4] (see Fig. 1). The relevant Hamiltonian is given by

$$H = -J \sum_{\langle i,j \rangle} a_i^\dagger a_j, \quad (1)$$

where $J > 0$ denotes the tunneling coupling of the electrons along the lattice sites, $\langle i,j \rangle$ denotes nearest neighbors and a_i^\dagger, a_i are the fermionic creation and annihilation operators at site i with the non-zero anticommutation relation $\{a_i, a_j^\dagger\} = \delta_{ij}$. The original lattice can be split into two triangular sublattices, A and B, that correspond to the black and blank circles in Fig. 1. This facilitates the evaluation of the dispersion relation of graphene, which is given by

$$E(p) = \pm J \sqrt{1 + 4 \cos^2 \frac{\sqrt{3}p_y}{2} + 4 \cos \frac{3p_x}{2} \cos \frac{\sqrt{3}p_y}{2}}, \quad (2)$$

where the distance between lattice sites is normalized to one. By solving the equation $E(p) = 0$ one deduces that, at half-filling, graphene possesses two independent Fermi points, denoted by \mathbf{K}_+ and \mathbf{K}_- , instead of Fermi lines. This rather unique property makes it possible to linearize its energy by expanding it near the conical singularities of the Fermi points. It is not hard to show that by restricting near the Fermi points the resulting Hamiltonian takes the form of the Dirac operator

$$H_\pm = \pm \frac{3J}{2} \gamma^\alpha p_\alpha, \quad (3)$$

where repeated indices are summed over the spatial coordinates x, y . The Dirac matrices, γ^α , are given by the Pauli matrices, $\gamma^\alpha = \sigma^\alpha$, and \pm corresponds to the two independent and oppositely positioned Fermi points. Hence, the low energy limit of graphene is described by a free fermion theory. Eigenstates of this Dirac operator are two dimensional vectors, called spinors, given by $(|\mathbf{K}_\pm A\rangle, |\mathbf{K}_\pm B\rangle)^T$, where A and B denote the two sublattices and \mathbf{K}_\pm denote two independent Fermi points chosen such that $\mathbf{K}_- = -\mathbf{K}_+$.

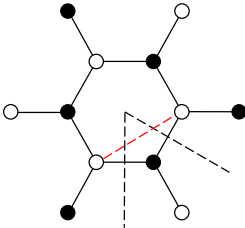


Fig. 1. The honeycomb lattice comprises of two triangular lattices, A, denoted by black circles and, B, denoted by blank circles. A single pentagonal deformation can be introduced by cutting a $\pi/3$ sector and gluing the opposite sites together.

3 Curvature deformations and effective gauge fields

Here we are interested in surfaces with arbitrary topology so we need to introduce curvature in the initially flat honeycomb lattice. This is achieved by selectively inserting lattice deformations. In doing so, we shall demand that each lattice site has exactly three neighbors and that the lattice is inextensional that is it is free to bend, but impossible to stretch. The minimal alteration of the honeycomb lattice that can introduce curvature without destroying the cardinality of the sites is the insertion of a pentagon or a heptagon; this corresponds to locally inserting positive or negative curvature, respectively. Other geometries are also possible, leading to similar results as we shall see in the following.

To introduce a single pentagon in a honeycomb lattice, one can cut a $\pi/3$ sector and glue the opposite sides together, as illustrated in Fig. 1. This causes no other defects in the lattice structure. We shall demand that the spinors are smooth along the cut remedied by introducing compensating fields which negate the discontinuity [5,6]. Indeed, the cut introduced in Fig. 1 causes an exchange between A and B sublattices. This discontinuity can be remedied by introducing in the Hamiltonian the non-abelian gauge field \mathbf{A} circulation

$$\oint A_\mu dx^\mu = \frac{\pi}{2} \tau_y \quad (4)$$

where τ_y is the Pauli operator that mixes the \mathbf{K}_+ and \mathbf{K}_- spinor components. This flux can be attributed to a fictitious magnetic monopole inside the surface with a charge contribution of $1/8$ for each pentagon [17]. In addition, moving a frame around the pentagonal deformation gives a non-trivial coordinate transformation. The effect of this transformation on the spinors can be described by a spin connection Ω . This is chosen such that its flux around the pentagon is given by

$$\oint \Omega_\mu dx^\mu = -\frac{\pi}{6} \sigma_z \quad (5)$$

and measures the angular deficit of $\pi/3$ around the cone.

The modified Dirac equation, which incorporates the curvature and the effective gauge field, couples the \mathbf{K}_\pm spinor components together due to the non-abelian character of \mathbf{A} . Since this is the only mixing term they can be decoupled by a single rotation that gives

$$\frac{3J}{2} \gamma^\mu (p_\mu - i\Omega_\mu - iA_\mu^k) \psi^k = E\psi^k, \quad (6)$$

where $k = 1, 2$ denotes the components in the rotated basis with the circulation of the abelian now field given by $\oint A_\mu^k dx^\mu = \pm\pi/2$ (no summation is considered in k). The curved space Dirac matrixes γ^μ are given by $\gamma^\mu = \sigma^\alpha e_\alpha^\mu$, where e_α^μ is the zweibein of the curved surface with metric $g_{\mu\nu}$ that defines the local flat reference frame, $\eta_{\alpha\beta} = e_\alpha^\mu e_\beta^\nu g_{\mu\nu}$. They satisfy the anti-commutation relations $\{\gamma^\mu, \gamma^\nu\} = 2g^{\mu\nu}$, where $g^{\mu\nu}$ is the inverse of $g_{\mu\nu}$. The curvature of the surface is given by the tensor

$$\mathcal{R}^\mu{}_{\nu\rho\sigma} = \partial_\sigma \Gamma_{\nu\rho}^\mu - \partial_\rho \Gamma_{\nu\sigma}^\mu + \Gamma_{\nu\rho}^\lambda \Gamma_{\lambda\sigma}^\mu - \Gamma_{\nu\sigma}^\lambda \Gamma_{\lambda\rho}^\mu$$

where the Christoffel symbols are defined by

$$\Gamma_{\mu\nu}^\sigma = \frac{1}{2} g^{\sigma\rho} (\partial_\mu g_{\nu\rho} + \partial_\nu g_{\mu\rho} - \partial_\rho g_{\mu\nu})$$

The Ricci tensor is given by $\mathcal{R}_{\mu\nu} \equiv \mathcal{R}^\sigma{}_{\mu\nu\sigma}$ and the scalar curvature is given by $\mathcal{R} \equiv g^{\mu\nu} \mathcal{R}_{\mu\nu}$. The field strength that corresponds to the abelian gauge potential, A_μ^k , is given by $\mathcal{F}_{\mu\nu}^k = \partial_\mu A_\nu^k - \partial_\nu A_\mu^k$. Equation (6) faithfully describes the low energy behavior of graphene, such as its zero modes, when it is deformed to an arbitrary surface.

4 Index theorem and graphene

4.1 The index theorem

Since the obtained Dirac operator is an elliptic operator, it is possible to employ the index theorem [7,8,9] to gain information about its low energy spectrum. Indeed, the index theorem gives an insight in the structure of the spectrum of certain operators without the need to diagonalize them. This information can be derived from general properties of the operators and the geometry of the space, M , they are defined on. A two dimensional Dirac operator defined on a surface coupled to a gauge field can be given by the general form

$$\mathcal{D} = \begin{pmatrix} 0 & P^\dagger \\ P & 0 \end{pmatrix}$$

where P is an operator that maps from a space V_+ to the space V_- , while P^\dagger maps from V_- to V_+ . As we are interested in the zero modes, we can define the dimension of the null subspace of P and P^\dagger by ν_+ and ν_- respectively. To facilitate the bookkeeping we introduce the chirality operator γ_5 by

$$\gamma_5 = \begin{pmatrix} 1 & 0 \\ 0 & -1 \end{pmatrix} = \sigma_z$$

so that it anticommutes with the Dirac operator and it has the states in V_\pm as eigenstates with corresponding eigenvalue ± 1 . As we are interested in the zero modes we can consider the operator \mathcal{D}^2 , which is diagonal

$$\mathcal{D}^2 = \begin{pmatrix} P^\dagger P & 0 \\ 0 & P P^\dagger \end{pmatrix}$$

and has the same number of zero modes as \mathcal{D} . One can easily show that the operators $P P^\dagger$ and $P^\dagger P$ have the same number of non-zero eigenstates. Indeed, if there is a state u such that $P P^\dagger u = \lambda u$ then the state $P^\dagger u$ is an eigenstate of the operator $P^\dagger P$ with the same eigenvalue, $P^\dagger P (P^\dagger u) = \lambda (P^\dagger u)$. In order to demonstrate the index theorem we shall employ the heat kernel expansion method [18]. Consider a two dimensional compact surface, M . Then one can consider the expansion

$$Tr(\hat{f} e^{-t\hat{D}}) = \frac{1}{4\pi t} \sum_{k \geq 0} t^{k/2} a_k(\hat{f}, \hat{D}) \quad (7)$$

where Tr denotes the trace of matrices and the integration of spatial coordinates. $a_n(\hat{f}, \hat{D})$ are the expansion coefficients that one needs to determine as a function of the operators \hat{f} and \hat{D} . For $\hat{f} = \gamma_5$ and $\hat{D} = \mathcal{D}^2$ one deduces that

$$Tr(\gamma_5 e^{-t\mathcal{D}^2}) = Tr(e^{-tP^\dagger P}) - Tr(e^{-tP P^\dagger}) = \sum_{(\lambda_1)} (e^{-t\lambda_1}) - \sum_{(\lambda_2)} (e^{-t\lambda_2})$$

where λ_1 and λ_2 are the eigenvalues of the operators $P^\dagger P$ or $P P^\dagger$ respectively. But we have shown that for every eigenstate of the operator $P^\dagger P$ there is a corresponding eigenstate of $P P^\dagger$ with exactly the same eigenvalue. Thus only the zero eigenvalues remain giving

$$Tr(\gamma_5 e^{-t\mathcal{D}^2}) = \nu_+ - \nu_-$$

Combining this result with relation (7) it is possible to deduce, that, for $f = \gamma_5$ and $D = \mathcal{D}^2$, all of the coefficients a_k should be zero except for a_2 where $a_2 = \nu_+ - \nu_- \equiv index(\mathcal{D})$. The value of a_2 defined from (7) can be found from the first order term in the t expansion of the exponential. Considering that $\mathcal{D}^2 = -g^{\mu\nu} \nabla_\mu \nabla_\nu + \frac{i}{4} [\gamma^\mu, \gamma^\nu] \mathcal{F}_{\mu\nu} - \frac{1}{4} \mathcal{R}$, where ∇_μ is the reparametrization and gauge covariant derivative, one can easily deduce that

$$a_2 = Tr \left[\gamma_5 \left(\frac{i}{4} [\gamma^\mu, \gamma^\nu] \mathcal{F}_{\mu\nu} - \frac{1}{4} \mathcal{R} \right) \right] = 2 \iint \mathcal{F}$$

where \mathcal{F} is the field strength, \mathcal{R} is the scalar curvature and the integration runs over the whole compact surface M . Thus, we have an analytic way to evaluate the index of \mathcal{D} by

$$\text{index}(\mathcal{D}) = \frac{1}{2\pi} \iint \mathcal{F} \quad (8)$$

The absence of the curvature term in this formula is due to the traceless nature of γ_5 and it is a characteristic of two dimensions. If one can evaluate the integral of the field strength over the whole compact surface then the least number of zero modes is determined. It is worth noting that for compact surfaces this integral is an integer due to the Dirac quantization condition of the monopole charges [17].

4.2 Application to graphene

Our aim is to evaluate the contribution from the gauge field, \mathcal{F} , in (8) for the particular case of a folded sheet of graphene in a compact surface. In a previous section we determined how for each lattice deformation a gauge field circulation is introduced. If one could determine the total number of deformations for a particular compact geometry of the lattice then we would be able to determine the $\text{index}(\mathcal{D})$. At this point we shall assume that curvature is introduced by only inserting pentagons and heptagons in the lattice. Interestingly, one can evaluate the number of such deformations in a lattice necessary to generate a compact surface by employing the Euler characteristic. Indeed, for V , E and F being respectively the number of vertices, edges and faces of a lattice defined on a compact surface with genus g , the Euler characteristic, χ , is given by

$$\chi = V - E + F = 2(1 - g). \quad (9)$$

Take the total number of pentagons, hexagons and heptagons in the lattice to be, n_5 , n_6 and n_7 , respectively. Then the total number of edges is given by $E = (5n_5 + 6n_6 + 7n_7)/2$ as each polygon n_i contributes i edges, but each edge is shared by two polygons. Similarly the total number of vertices and faces can be evaluated to be $V = (5n_5 + 6n_6 + 7n_7)/3$ and $F = n_5 + n_6 + n_7$, giving finally

$$n_5 - n_7 = 12(1 - g). \quad (10)$$

This result signifies that non-trivial topologies necessarily introduce an imbalance in the numbers of pentagons and heptagons. Moreover, inserting equal numbers of pentagons and heptagons do not change the topology of the surface as they cancel out. This is consistent with the effective gauge field description where a pentagon and a heptagon have opposite flux contributions. As particular examples we see that Eqn. (10) reproduces the known case of a sphere with $g = 0$ giving $\chi = 2$ and a number of defects $n_5 = 12$ and $n_7 = 0$. This is the lattice of the C_{60} fullerene. For the torus we have $g = 1$ for which $\chi = 0$ and $n_5 = n_7 = 0$ reproducing the lattice of the nanotubes. For a genus-2 surface we have $\chi = -2$, $n_5 = 0$, $n_7 = 12$. In all these examples equal numbers of pentagons and heptagons can be inserted without changing the topology of the surface.

Now we are in position to evaluate the $\text{index}(\mathcal{D})$. The contribution of the gauge field term in (8) can be calculated straightaway from the Euler characteristic. It is obtained by adding up the contributions from the surplus of pentagons or heptagons. Thus, the total flux of the effective gauge field can be evaluated by employing Stokes's theorem, giving

$$\frac{1}{2\pi} \iint \mathcal{F} = \frac{1}{2\pi} \sum_{n_5 - n_7} \oint A = \frac{1}{2\pi} (\pm \frac{\pi}{2})(n_5 - n_7) = \pm 3(1 - g), \quad (11)$$

where the sign \pm corresponds to the $k = 1, 2$ gauge fields and the summation runs over all the surplus of pentagons or heptagons. Hence, from (8), one obtains

$$\text{index}(\mathcal{D}) = \nu_+ - \nu_- = \begin{cases} 3(1 - g), & \text{for } k = 1 \\ -3(1 - g), & \text{for } k = 2 \end{cases} \quad (12)$$

Consequently, the least number of zero modes is given by $6|1 - g|$, which coincides with their exact number if $\nu_- = 0$ or $\nu_+ = 0$. This is actually what happens in most of the cases when the index is non-zero.

4.3 Zero modes for fullerenes and nanotubes

The above result relates the number of zero modes of a graphene sheet with the genus of the surface it has been folded. As expected it reproduces the number of zero modes for the known molecules. The fullerene, for which genus $g = 0$, has six zero modes which correspond to the two triplets of C_{60} and of similar larger molecules [4,19]. For the case of nanotubes, we consider periodic boundary conditions, which give effectively a torus with $g = 1$. In this case, formula (12) gives $\nu_+ - \nu_- = 0$. This is in agreement with previous theoretical and experimental results [20,11] which have the nanotubes with either no zero modes (e.g. zigzag nanotubes) or with zero modes that satisfy $\nu_+ = \nu_-$ (e.g. armchair nanotubes). This is a consequence of the symmetry between the two opposite directions along the nanotube.

5 Conclusions

In this article we have employed the index theorem [7] to enumerate the zero modes of a graphene sheet when compactified on arbitrary genus surfaces. Our results are in good agreement with the presently studied cases of fullerenes and nanotubes. The only approximation employed here was the continuous limit for obtaining the Dirac operator. This approximation is valid if we restrict to the low energy spectrum of the system described by large wavelengths. In this limit, the lattice spacing or the conical singularities of the pentagonal deformations do not affect the low energy modes. Thus, larger fullerene molecules than the C_{60} provide more accurate results.

As an additional example we can consider a graphene sheet folded on an octahedron. In this case six square plaquettes have to be inserted in the honeycomb lattice. As square plaquettes do not have the frustration properties of pentagons, no effective gauge field is introduced. Thus, the index in this case is zero, agreeing with previous considerations [4]. Beyond the known examples the version of the index theorem presented here gives a relation between the zero modes of more complex molecules. Even if the latter are defined on compact surfaces they are related to experimentally relevant ones by imposing appropriate periodic conditions. Thus, the metallic properties of these molecules can be induced by simple geometrical considerations.

This research was supported by the Royal Society.

References

1. D. P. DiVincenzo and E. J. Mele, Phys. Rev. B **29**, (1984) 1685.
2. J. Tworzydło, B. Trauzettel, M. Titov, and C. W. Beenakker, cond-mat/0603315.
3. J. González, F. Guinea, and M. A. Vozmediano, Phys. Rev. Lett. **69**, (1992) 172.
4. J. González, F. Guinea, and M. A. Vozmediano, Nucl. Phys. B **406** (1993) 771.
5. P. E. Lammert, and V. H. Crespi, Phys. Rev. Lett. **85**, 5190 (2000); Phys. Rev. B **69**, (2004) 035406.
6. D. V. Kolesnikov and V. A. Osipov, Eur. Phys. J. B **49**, (2006) 465 ; V. A. Osipov, E. A. Kochetov, JEPT **73**, (2001) 631.
7. M. F. Atiyah and I. M. Singer, Ann. of Math. **87**, (1968) 485; Ann. of Math. **87**, (1968) 546; Ann. of Math. **93**, (1971) 119; Ann. of Math. **98**, (1971) 139; M. F. Atiyah and G. B. Segal, Ann. of Math. **87**, (1968) 531.
8. T. Eguchi, P. B. Gilkey, and A. J. Hanson, Phys. Rep. **66**, (1980) 215.
9. M. Stone, Ann. Phys. **155**, (1984) 56.
10. H. W. Kroto, J. R. Heath, S. C. O'Brien, R. F. Curl and R. E. Smalley, Nature **318**, (1985) 162; R. F. Curl and R. E. Smalley, Sci. Am. **265**, (1991) 54.
11. S. Reich, C. Thomsen, and P. Ordejón, Phys. Rev. B **65**, (2002) 155411.

12. G. W. Semenoff, Phys. Rev. Lett. **53**, (1984) 2449.
13. A. M. J. Schakel and G. W. Semenoff, Phys. Rev. Lett. **66**, (1991) 2653.
14. R. Jackiw, Phys. Rev. D **29**, (1984) 2375.
15. X. G. Wen and Q. Niu, Phys. Rev. B **41**, (1990) 9377.
16. M. Alimohammadi, and H. M. Sadjadi, J. Phys. A: Math. Gen. **32**, (1999) 4433.
17. S. Coleman, *The Magnetic Monopole Fifty Years Later*, in *The Unity of the Fundamental Interactions* (Plenum Press, New York, 1983).
18. D.V. Vassilevich, Phys.Rept. **388** (2003) 279-360.
19. S. Samuel, Int. J. Mod. Phys. B, **7**, (1993) 3877.
20. R. Saito, M. Fujita, G. Dresselhaus, and M. S. Dresselhaus, Phys. Rev. B **46**, (1992) 1804.